2026 IEEE/SICE International Symposium on System Integration (SII)
January 11-14, 2026. Cancún, México

Motion Planning Leveraging High-Speed Sensors for Conventional Industrial Manipulator

Misato Koreki, Usukhbayar Chuluunbat, Hikaru Arita, Kazuto Nakashima, and Kenji Tahara

Abstract— **High temporal resolution sensors have become increasingly widespread in recent years, enabling detailed and accurate observation of fast physical phenomena and contributing to the understanding of their essential properties. However, a fundamental challenge remains in bridging the temporal resolution gap between such sensors and conventional industrial robots. Typical high-speed visual feedback control require all system components to operate at high speed, inherently restricting their applicability to phenomena within the robot's dynamic capabilities. As a result, valuable high-speed sensing data often cannot be fully utilized, especially when target phenomena evolve faster than the robot can respond. This study proposes a novel motion planning method that extracts essential, task-relevant information from high-speed sensor data to bridge the timescale gap between sensors and robots. Based on the extracted information, feedforward control is executed with consideration of the robot's motion characteristics. To explore practical solutions, we developed an integrated system combining a high-speed camera and a proximity sensor module —both with existing applications in robotics—with a general-purpose industrial robot and gripper. A case study involving the grasping of a pendulum-swinging object by a low-speed robot demonstrates the effectiveness of the proposed approach in utilizing high-frequency measurements for tasks beyond the limits of conventional feedback control.**

I. INTRODUCTION

In recent years, various sensors—including vision, proximity, tactile, and acceleration sensors—have undergone significant improvements in spatiotemporal resolution, alongside miniaturization and cost reduction. Consequently, these sensors have become widely utilized as more common and versatile measurement tools in both industrial and research fields.

Since sensor-based measurements are performed as discrete sampling at specific time points, it is fundamentally difficult to obtain complete time-series information for phenomena where physical quantities change continuously. Therefore, when the sensor's sampling frequency is insufficient compared to the rate of change of the target phenomenon, aliasing may occur, causing the measurement data to misrepresent the actual phenomenon. For this reason, higher temporal resolution of sensors enables more accurate and detailed capture of phenomena.

For example, high-speed vision sensors, which provide high temporal resolution visual data, are utilized for purposes such as monitoring, analysis, and anomaly detection by leveraging their detailed time-series information. Specifically, in cell swimming tracking (1 kHz) [1] and random object tracking in dynamic environments (0.5 kHz) [2], it has become possible to identify and track the position and motion of target objects from visual data in real-time. Additionally, in applications such as observation of chip particle formation during machining processes (5 kHz) [3] and visualization of plasma spraying phenomena (0.3 MHz) [4], the mechanisms of complex processes have been elucidated and stability evaluations have been conducted. In this manner, sensors with high temporal resolution can capture steep and instantaneous changes without omission, potentially leading to understanding of essential properties such as structural characteristics and causal relationships of phenomena, rather than merely their apparent features. Therefore, effective utilization of high-speed measurement information in robot operation may lead to improvements in safety, efficiency, and autonomy in various applications and environments.

High-speed visual feedback control is a typical application of high temporal resolution sensors in robotics. This is a representative method that directly utilizes visual information obtained from high-speed cameras for robot control [5]–[7], aiming to respond flexibly and robustly to rapid changes in dynamic environments. These methods require robots capable of high-speed operation appropriate to the target task. For example, methods have been proposed that react to dynamic objects in human environments using an end-effector with a maximum speed of 6 m/s and a 1 kHz vision system [5], [6], and systems that recognize human gestures at 1 kHz and operate robot hands at a maximum speed of 4.5 m/s [7]. In this way, by directly utilizing information from high-speed sensors for feedback, robots can respond immediately to changes in the external environment. However, in such feedback control schemes, the range of target dynamics that can be effectively addressed is inherently limited by the motion capabilities of the robot. Therefore, for robots to respond to high-speed phenomena, lightweight structures with high acceleration and high precision are required, but robots with such specifications have not become widespread from the perspectives of versatility and cost. Although methods for adding compensation modules to general robots have also been proposed [8], these are also specialized for specific applications and have not achieved widespread adoption. Furthermore, robot motion speed has limitations due to constraints in mechanical structure and drive systems. However, sensors operate much faster than robots with potential for further speed increases, and the

*This work was partially supported by JSPS KAKENHI Grant Number JP24H00726.

The authors are with Department of Mechanical Engineering, Kyushu University, Fukuoka 819-0395, JAPAN (e-mail: [koreki, uskha]@hcr.mech.kyushu-u.ac.jp; [arita, kazuto, tahara]@ieee.org).

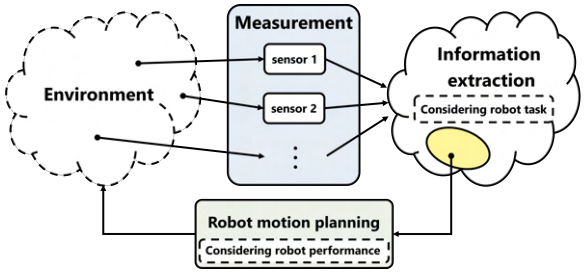

Fig. 1: The concept of the proposed method

timescale difference between robots and sensors is expected to continue widening. Therefore, methods that can maximize the utilization of high-speed measurement information in robot operation are necessary.

In this paper, we propose a motion planning method that extracts essential information from high-speed measurement data obtained by high temporal resolution sensors, considering the motion characteristics of the robot. The key aspect of the proposed approach lies in the extraction of information that bridges the temporal scale gap between the sensor and the robot. By incorporating feedforward control based on the robot's motion capabilities, the method enables appropriate responses even when there is a significant timescale mismatch between the physical phenomenon and the robot.

The system used in this study is composed of commercially available components: a high-speed camera and a proximity sensor—both of which have existing use cases in robotic applications [5]–[7], [9]—combined with a standard collaborative robot and gripper. Using this system, we develop a concrete method to effectively leverage high-speed measurement data. A case study is conducted in which a low-speed robot attempts to grasp a pendulum-swinging object. First, through experiments using only measurement information from high-speed cameras, we demonstrate that the proposed method enables robots to grasp objects moving faster than the robots themselves. Furthermore, we show that task accuracy improves by integrating information from high-speed cameras and proximity sensors.

II. THE PROPOSED INTEGRATING SYSTEM

The concept of the proposed method is illustrated in Fig. 1. The core idea of this method is to enable motion planning that is independent of the timescale gap between the sensors and the robot, by fully utilizing the high-speed capabilities of sensors to accurately measure and analyze physical phenomena. The proposed method is mainly divided into three steps: 1) the measurement step, 2) the information extraction step, and 3) the motion planning step.

In the measurement step, the measurement process is decoupled from the robot's motion planning, and the target phenomenon is measured at the maximum measurement rate. Furthermore, each sensor operates independently within the measurement step, without mutual dependence in sampling rate. This architecture allows the flexible integration of multiple sensors according to the characteristics of the target phenomenon, while maintaining the high-speed capabilities of each sensor.

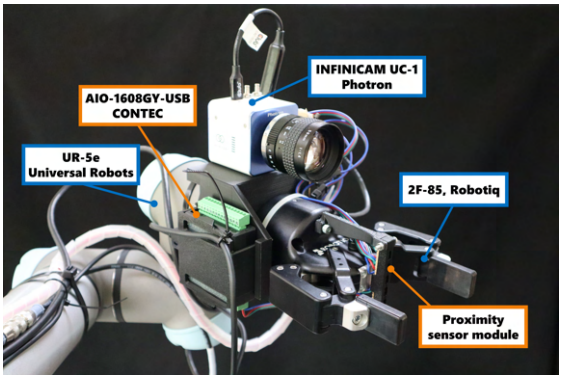

Fig. 2: End-effector of the industrial robot

Next, in the information extraction step, the information obtained in the measurement step is processed to extract task-relevant information. This step is independent from the sensor sampling rate or the robot servo loop, and serves to bridge the time-scale gap between the sensors and the robot. Each sensor's information is used to analyze the essential features of the target phenomenon, and the results of this analysis are key to generating an optimal trajectory for the robot, which moves at a relatively low speed compared to the phenomenon.

Finally, in the motion planning step, motion planning is performed based on the extracted information, taking into account the robot's physical limitations, and the robot is controlled according to the resulting trajectory. The generated trajectory is designed with consideration of constraints such as minimum execution time, workspace boundaries, and computational delays. This enables the robot to appropriately respond to the target phenomenon, even if its motion speed is relatively low compared to the dynamics of the phenomenon.

III. INTEGRATED SYSTEM FOR GRASPING FAST-MOVING OBJECTS

A. System configuration

Fig. 2 shows the configuration of the robot end-effector developed based on the proposed method. We built a system by attaching a gripper (2F-85, Robotiq), a high-speed streaming camera (INFINICAM UC-1, Photron), a proximity sensor module, and an analog-input USB I/O unit (AIO-1608GY-USB, CONTEC) to an industrial robotic arm (UR5e, Universal Robots). The measurement rate is set to 1 kHz for both the high-speed camera and the I/O unit. The system is designed for grasping fast-moving objects using an industrial robot.

First, the high-speed camera is used to capture the target phenomenon, enabling the robot to approach it. However, high-speed cameras inherently involve a trade-off between resolution and processing time; maintaining high resolution during high-speed recording results in a limited field of view. To address this, a hand-eye system is adopted to ensure a flexible measurement area. Since the focal length

of the high-speed camera is fixed, it becomes difficult to perform measurement once the robot begins approaching the phenomenon.

To perform secondary measurement after the robot has approached the target, we introduced a proximity sensor. To precisely measure the object as it passes through the gripper, we adopted an infrared reflective photo-reflector (RPR-220, ROHM), which is compact, high in temporal resolution, and suitable for distribution over the gripper surface. The design of the proximity sensor module is based on the Net-Structure Proximity Sensor (NSPS) proposed by Hasegawa et al. [10], in which multiple sensor elements are connected via a resistive network to achieve high-speed response and object center position prediction. The proximity sensor module consists of two parts: a sensor element unit (six RPR-220 units spaced at 10 mm intervals) and a computation circuit unit, mounted on the gripper palm and the robot wrist, respectively. The computation circuit sums and distributes the current from each phototransistor and calculates the voltage difference $V_1 - V_2$ at both ends as the first-order moment to determine the object's center of gravity relative to the center of the sensor. Accordingly, the I/O unit is used to sample V_1 and V_2.

B. A case study

To validate the effectiveness of the proposed method, we conducted an experiment in which an industrial robot grasps a pendulum-swinging object. Spatiotemporal information obtained from a high-speed camera and the proximity sensor module is used to extract the characteristics of the pendulum, including its period. The robot then approaches the object and attempts to grasp it using a two-fingered gripper. Since this gripper cannot perform high-speed grasping, its response time must be taken into account, requiring precise prediction of the grasping point in both spatial and temporal dimensions.

The success rate of the task is significantly influenced by the point along the pendulum's trajectory where the grasp is attempted. For instance, at the lowest point of the swing, the object velocity is highest, making prediction errors critical to grasp success. Thus, grasping at the equilibrium point (i.e., the lowest point) is the most challenging. To demonstrate the effectiveness of the proposed method, we intentionally set the grasping point to the equilibrium position, where tolerance for prediction error is minimal.

To accurately analyze the pendulum's behavior, high-resolution spatiotemporal information is required. Using a low temporal resolution sensor to capture a fast phenomenon would not yield sufficiently precise information. However, both the high-speed camera and the proximity sensor module used in this study offer high temporal resolution and are capable of providing the data needed to estimate pendulum characteristics. As a result, they allow for accurate detection of the exact lowest point of the pendulum swing, which is not possible with low-resolution sensors. Therefore, this problem setup represents a simple example of a phenomenon that can only be measured using high temporal resolution sensors. Moreover, the pendulum system is structurally simple and easy to experiment with, and the experiment can be conducted under varying conditions by altering the string length, mass, and initial position.

This paper introduces two experiments: one using only the high-speed camera, and another integrating data from both the high-speed camera and the proximity sensor module. In the first experiment using only the high-speed camera, the object is captured as it passes through the lowest point, and the half-period and location of the pendulum swing are measured. Using this periodic information, the future time at which the object will again pass the lowest point is predicted. Then, considering the time required for the robot to approach the object, relevant constraints, and the inherent motion time of the gripper, an optimal motion plan is generated. The robot is moved to the predicted trajectory of the pendulum, and the gripper is activated in advance so that it is ready by the time the object reaches the lowest point—making it possible for a slow robot to grasp a fast-moving object.

In the second experiment, the proximity sensor module is used to refine the timing of the grasping point predicted from the high-speed camera. After the robot has approached the object based on the high-speed camera data, the proximity sensor mounted on the gripper palm measures the actual moment when the object passes through the gripper. This measurement is then used to correct the previously predicted grasping time. Finally, the corrected information is used to determine the precise timing at which to begin the grasping motion, taking into account the gripper's response time.

The proposed concept applied in the case study is summarized as follows:

Information acquisition
: Position of the pendulum ball

Information extraction
: prediction of the pendulum period and catching candidate points

Prediction for robot motion
: Determination of the catch point

Robot task
: Grasping a fast-moving object

IV. GRASPING MOTION PLANNING CONSIDERING ROBOT PERFORMANCE

A. Prediction of the transition of catching candidate points

Let the position of the equilibrium point be denoted by p_n and the time at which the object passes through the equilibrium point be denoted by T_n. Here, n is a natural number, where $n = 1$ corresponds to the first measurement acquired by the high-speed camera, and n represents the number of times the object has passed through the equilibrium point. Measurements at $n = 1, 2$ are obtained using a high-speed camera. Based on the two measured equilibrium point passage times, T_1 and T_2, the half-period of the pendulum motion is computed as $T_p = T_2 - T_1$. Accordingly, the predicted grasping candidate time T_N is given by:

$$T_{\mathrm{N}} = T_2 + (N-2)T_{\mathrm{p}}. \tag{1}$$

The parameter N is selected in consideration of the robot's kinematic constraints. The required time for the robot to reach the grasping point, denoted by T_{op}, is expressed as:

$$T_{\mathrm{op}} = (N - n)T_{\mathrm{p}}. \tag{2}$$

B. Consideration of the robot workspace range and execution time

In this section, the catching point and time are evaluated using the robot kinematic constraint and execution time. To evaluate the robot's motion time, the trajectory must first be planned. To ensure smooth trajectory execution and avoid computational complexity, the following quintic polynomial is utilized. In addition, we plan the trajectory in joint space to prevent any issues that may arise from kinematic singularities.

$$q_i(t) = \sum_{j=0}^{5} a_j t^j, t \in [0, T_{\mathrm{r}}], \tag{3}$$

where $i = 1 \dots m$ is the joint index of the m-DoF robot, q_i is the joint position, t is the time and T_{r} refers to the total time of robot motion execution. Additionally, $a_j, (j = 0, \cdots, 5)$ is constant and can be calculated by considering the boundary condition as follows:

$$\text{Initial state} \quad t = 0 : \boldsymbol{q}_{\mathrm{init}}, \dot{\boldsymbol{q}}_{\mathrm{init}}, \ddot{\boldsymbol{q}}_{\mathrm{init}}, \tag{4}$$

$$\text{Final state} \quad t = T_r : \boldsymbol{q}_{\mathrm{f}}, \dot{\boldsymbol{q}}_{\mathrm{f}}, \ddot{\boldsymbol{q}}_{\mathrm{f}}. \tag{5}$$

Based on this boundary condition, we first utilize the robot's inverse kinematics to compute $\boldsymbol{q}_{\mathrm{f}}$ based on the pose and orientation of the end-effector $\boldsymbol{p}_N$. If $\boldsymbol{q}_{\mathrm{f}}$ has no solution, meaning that $\boldsymbol{p}_N$ is predicted to be outside the robot's workspace (W), then the catch task cannot be performed. Therefore, the prediction process is repeated until $\boldsymbol{p}_N$ is found within the workspace.

Once $\boldsymbol{q}_{\mathrm{f}}$ is found, we consider the kinematic constraints, including the position, velocity, and acceleration limits for all joints, and find the minimum execution time. Hence, the optimal trajectory planning problem can be formulated as follows:

$$\min_{a_j} \quad T_r \tag{6a}$$

$$\text{s.t.} \quad |q_i(t)| \leq {q_i}^{\max}, \tag{6b}$$

$$|\dot{q}_i(t)| \leq \dot{q}_i^{\max}, \tag{6c}$$

$$|\ddot{q}_i(t)| \leq \ddot{q}_i^{\max}. \tag{6d}$$

Here, ${q_i}^{\max}, \dot{q}_i^{\max}, \ddot{q}_i^{\max}$ are the safety limits of the joint position, velocity, and acceleration, respectively. The minimum execution time is calculated while considering (3)-(6). Since T_{r} is calculated at each joint, the largest value is assumed to be representative. As mentioned above, the response time of the gripper is also considered in the prediction of the time for catching. Assuming that the response time of the gripper is known (T_{gr}), the minimum execution time for catching is expressed as follows:

$$T_{\mathrm{th}} = T_{\mathrm{r}} + T_{\mathrm{gr}} + T_{\mathrm{com}}, \tag{7}$$

where T_{com} refers to the computation time taken for the prediction and planning processes. The catching point and time can be evaluated by treating (T_{th}) as a threshold.

C. Re-prediction of catching candidate points based on proximity information

The proximity sensor is mounted such that its center aligns with the center of the gripper. As a result, $V_1 - V_2$ can be interpreted as the relative position of the object with respect to the gripper center. When the object is aligned with the sensor center (i.e., the gripper center), the response distribution of the six sensing elements becomes symmetric about the center, yielding $V_1 - V_2 = 0$. Therefore, the time at which $V_1 - V_2 = 0$ is estimated using linear interpolation, and the grasping point T_N is measured based on the proximity sensor readings. Subsequently, the future time at which the object is expected to pass through the gripper center is re-predicted as $T_{N'}$ by adding $N'T_p$ to T_N, where N' is a natural number:

$$T_{\mathrm{N}'} = T_N + N'T_p. \tag{8}$$

The parameter N' is evaluated using the gripper operation time T_{gr} as a threshold. In the conducted experiments, the gripper operation time T_{gr} was empirically set to 0.39 s.

V. EXPERIMENTS

A. Experimental setting

In this experiment, we conducted a grasping task using the system described in Section III-A, with the objective of performing the grasp at the moment when a pendulum-swinging object reached its equilibrium point (lowest point). To compare task performance, two experiments were conducted: Experiment 1, which utilized only a high-speed camera, and Experiment 2, which employed both the high-speed camera and the proximity sensor module. A golf ball with a diameter of 45 mm was used as the target object for the pendulum motion. The camera was configured with a frame rate of 1000 fps, a shutter speed of 1/2000 s, and a resolution of 1246 $\times$ 1008, and it was used to capture the object as it passed near the lowest point. The sampling rate of the proximity sensor module was set to 1 kHz, enabling the measurement of the object as it passed through the gripper. The pendulum-swinging object was grasped using a gripper equipped with fingertips of 22 mm in width. The gripper was operated under the conditions of a fingertip speed of 100 mm/s and a grasping force of 200 N. Control was conducted within the safe operating range of the UR5e robotic arm, taking into account its kinematic constraints. The kinematic limitations of the UR5e are as follows: the maximum range of motion for each joint is 180deg, the maximum joint speed is 90 deg/s, and the maximum joint acceleration is 90 deg/s². To simplify motion analysis, the pendulum motion was assumed to be two-dimensional, and the depth direction distance was predicted using the ball's radius and calibration. The position of the ball was obtained using a circle detection algorithm based on image processing.

TABLE I: Various experimental values

Evaluation Item	Ex. 1	Ex. 2
Measured Period	0.660 s	0.673 s
Predicted Catching Point Time	5.940 s	6.057 s
Measured Catching Point Time	—	6.037 s
Re-predicted Catching Point Time	—	6.710 s
Success Rate of Grasping Task (trials: 20)	30 %	40 %

The time-series data of the ball's motion were acquired based on the frame numbers of the camera.

B. Results

A sequence of images from the pendulum grasping experiment is shown in Fig. 3. Although Fig. 3 pertains to Experiment 2, the sequence up to Fig. 3(e) is identical to that of Experiment 1. The ball is released from the initial position, and camera recording begins (Fig. 3(a)). Subsequently, two instances of the equilibrium point are measured (Fig. 3(b), 3(c)), and the position and period of the ball's oscillation are calculated to estimate the catching point. The robot then moves to the predicted catching point.

In Experiment 1, the robot reaches the predicted pre-grasping position, and the gripper is activated to grasp the ball. In Experiment 2, after reaching the predicted pre-grasping position (Fig. 3(e)), the proximity sensor module begins sampling (Fig. 3(f)). The module measures the timing of the catching point, which was predicted based on high-speed camera data. After this measurement, the catching point is updated based on the proximity data, and the grasping action is initiated. As shown in Fig. 3(h), the gripper successfully grasps the ball, completing the grasping task.

In both Experiment 1 and 2, the robot moves to the predicted position before the ball arrives and begins gripper control(Fig. 3(g)). The gripper motion is controlled so that the ball and gripper reach the predicted position simultaneously. Ultimately, the gripper grasps the ball, successfully completing the task.

Figs. 4 and 5 show the measured and predicted positions of the ball, as well as the position of the robot's end-effector. Both graphs represent 3D trajectories, composed of the Y- and Z-coordinates of the position vector in the robot base coordinate system, together with the time vector referenced to the moment when the equilibrium point was first measured by the high-speed camera. The black and red dots both indicate the object measured by the camera, representing respectively the measured points and the extracted equilibrium points mapped to the robot base coordinate system. The blue dots shows the trajectory of the gripper's grasping position. The gripper trajectory exhibits an S-shaped path due to an waypoint that enables approaching from below the pendulum trajectory, avoiding perpendicular approach to the swing plane that would risk collision with the pendulum. The catching point predicted from the high-speed camera measurements is shown as a green dot, whose YZ-coordinates correspond to the mean position of the two measured equilibrium points. In Fig. 5, the yellow square indicates the catching point actually measured by the proximity sensor module, while the pink cross indicates the catching point re-predicted based on the measured catching point.

Table I presents the values measured by each sensor and the predicted timings. In Experiment 2, the predicted catching point and the measured catching point occur at times 6.057 s and 6.037 s, respectively, showing a difference of 0.02 s. The pendulum period calculated using the high-speed camera was approximately 0.673 s, and this value was used to update the timing of the catching point to 6.710 s.

To compare the grasping success rates between Experiment 1 and Experiment 2, each experiment was conducted 20 times. Experiment 1 achieved a success rate of 30 % (6 out of 20 trials), whereas Experiment 2 achieved a success rate of 40 % (8 out of 20 trials).

VI. DISCUSSION

A. Summary and interpretation of results

In Experiment 1, successful grasping was achieved using only visual information from the high-speed camera. There was a time gap of approximately 5 s between the measurement by the high-speed camera and the actual completion of the grasp. In feedforward control, such a delay can lead to the accumulation of significant errors. Nevertheless, grasping was possible because the high temporal resolution of the high-speed camera enabled accurate prediction of the equilibrium point and the pendulum period, which allowed long-term prediction based on this information. In other words, high temporal resolution sensing directly contributes to improving the accuracy of catching point prediction.

In Experiment 2, in addition to the high-speed camera, the proximity sensor module was introduced to perform re-measurement near the catching point. As a result, the grasping success rate improved by 10 % compared to Experiment 1. This improvement is considered to be due to the proximity sensor module enabling the measurement of the actual time at which the object passes the catching point, thereby reducing the prediction errors caused by long-term estimation.

On the other hand, the success rate remained limited, at 30 % for Experiment 1 and 40 % for Experiment 2 over 20 trials. One of the main reasons was that the effective frame rate of the high-speed camera decreased to approximately 500 Hz due to processing delays, despite being set to 1 kHz. This reduction causes the true equilibrium point position to be buried between frames, introducing millimeter-scale position errors that affected both catching point prediction and period estimation. To shorten the processing time, strategies such as reducing the object size to limit the search range or optimizing the setting of the search region would be effective. Another factor is gripper response time variability (millisecond-order), which significantly affects success when the pendulum passes at high speed.

Furthermore, insufficient prediction accuracy in the depth direction was also a cause of failure. The high-speed camera estimated the position based on the object radius, while the proximity sensor module could only obtain a one-dimensional component as the object passed through the

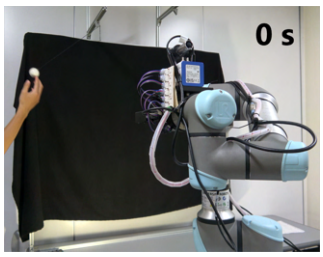

(a) The pendulum ball is released

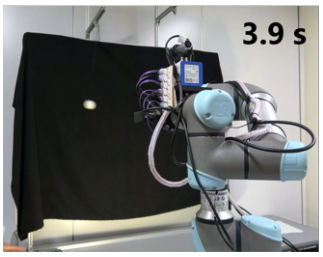

(b) 1st peak measurement by high-speed camera

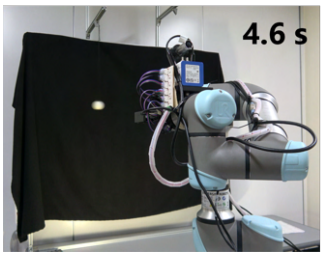

(c) 2nd peak measurement by high-speed camera

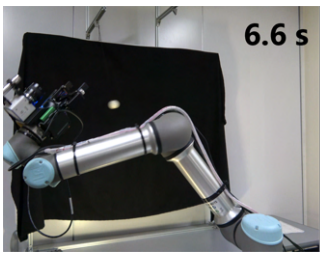

(d) Robot operating

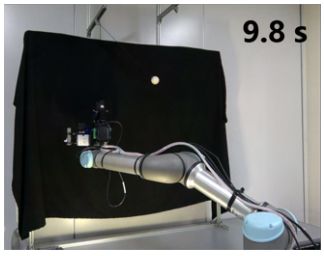

(e) Robot reaches catching point

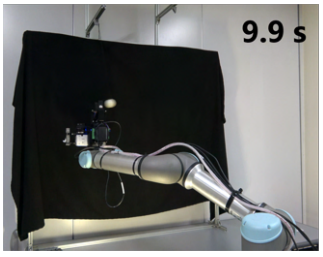

(f) Catching point measurement by proximity sensor module

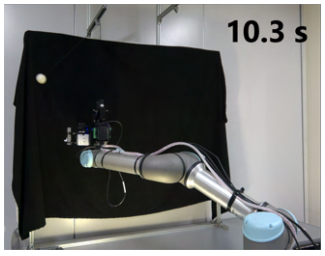

(g) Gripper motion started

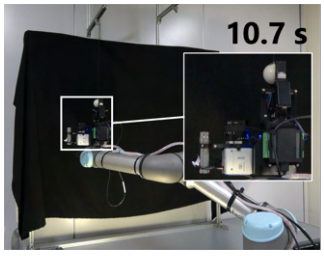

(h) Catching task ended

Fig. 3: States of the robot arm when catching a pendulum ball

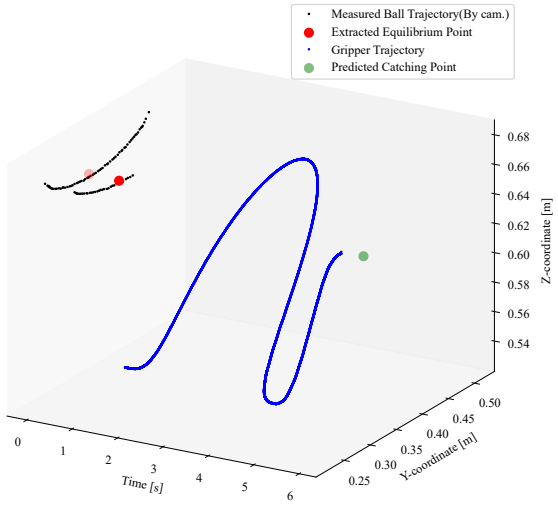

Fig. 4: Time histories of the ball and gripper position (Experiment 1)

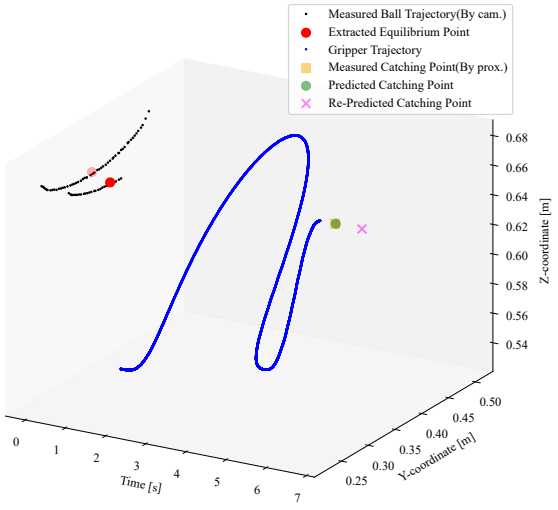

Fig. 5: Time histories of the ball and gripper position (Experiment 2)

gripper, making depth errors unavoidable. Additionally, uncalibrated optical characteristic variations among the RPR-220 sensors may have caused zero-crossing point deviations, introducing systematic errors. This issue could be mitigated by redesigning the proximity sensor module to acquire depth-direction spatial information, thereby enabling not only temporal correction of the catching point but also correction of its depth position, which could further improve the success rate.

B. Comparison with conventional high-speed feedback methods

The limitations of conventional high-speed feedback control [5]–[7] become particularly evident when applied to the pendulum grasping task investigated in this study. Near the equilibrium point of the pendulum, where the object velocity reaches its maximum, the speed of the object often exceeds the maximum velocity of the robot. In such situations, direct tracking through conventional feedback is practically infeasible. Moreover, in order to match the pendulum's dynamic acceleration profile, the robot must frequently execute high-

acceleration motions, which can result in instability and excessive energy consumption.

In contrast, the proposed method explicitly considers the slow dynamic characteristics of the robot and predicts the catching point based on the periodicity of the phenomenon, thereby generating feasible trajectories. In other words, even when direct tracking is infeasible, grasping can be achieved through predictive motion planning. In addition to precise measurement and future-state prediction enabled by high temporal resolution sensing, the framework allows multiple sensors to be utilized at their maximum measurement rate, providing extensibility. Consequently, by combining sensors appropriately according to the task, further improvements in task accuracy can be expected.

The proposed method is applicable when the target phenomenon exhibits predictable structures such as periodicity. Specifically, it is suitable for cases where (1) time-series sensor data enable prediction of essential characteristics or future behavior, (2) tasks are executable within the workspace, and (3) required interaction moments are reachable. Notably, future prediction is not always required; the framework can also be applied when high-speed sensing is used to predict the current state for motion planning—for example, coating tasks where droplet rebound observation is used to predict film thickness. Typical applicable scenarios include periodic or repetitive motions, such as objects on conveyors, rotating parts, or bouncing balls, where high temporal resolution enables precise characterization for planning.

Nevertheless, the proposed method still relies on the assumption that the target phenomenon possesses predictable or observable structures. Therefore, its applicability is limited in situations where such prior knowledge is unavailable or where high-speed sensing cannot extract task-relevant information, such as completely opaque processes or tasks with unclear relationships between observed phenomena and required actions. Despite these limitations, the framework retains high versatility and has the potential to demonstrate further effectiveness when applied to faster and more complex dynamic phenomena.

VII. CONCLUSION

This study proposed a motion planning method that bridges the timescale gap between high-speed sensors and robots by introducing an intermediate information-extraction step between environmental measurement and robot motion planning, in contrast to conventional high-speed feedback control approaches.

Following the proposed methodology, we developed an integrated system comprising a high-speed camera, a proximity sensor module, and a conventional industrial robot. As a case study, we applied this integrated system to the task of grasping a pendulum-like moving object. In accordance with the proposed method, we extracted periodic motion information from high-speed measurement data as the form of task-relevant information necessary for grasping. Motion planning was then carried out with consideration of the dynamic characteristics of a slow-moving robot, resulting in successful grasping. This demonstrated that the proposed approach enables reliable task execution even when the robot operates at a lower speed than the observed phenomenon.

Furthermore, we compared two experiments: one using only the high-speed camera (Experiment 1) and another using both the high-speed camera and the proximity sensor module (Experiment 2). The task success rate in Experiment 2 was 10 % higher than in Experiment 1. This confirms that, depending on the task, combining or adding sensors can improve task accuracy.

As future work, we aim to extend the proposed framework to handle tasks involving faster and more complex dynamic phenomena, thereby further demonstrating its versatility.

REFERENCES

[1] K. Yamato, H. Chiba, and H. Oku, "High speed three dimensional tracking of swimming cell by synchronous modulation between tece camera and tag lens," *IEEE Robot. Autom. Lett.*, vol. 5, no. 2, pp. 1907–1914, Apr. 2020.

[2] M. Jiang, K. Shimasaki, S. Hu, T. Senoo, and I. Ishii, "A 500-fps pan tilt tracking system with deep-learning-based object detection," *IEEE Robot. Autom. Lett.*, vol. 6, no. 2, pp. 691–698, Apr. 2021.

[3] Y. Guo, W. D. Compton, and S. Chandrasekar, "In situ analysis of flow dynamics and deformation fields in cutting and sliding of metals," *Proc. Roy. Soc. A*, vol. 471, no. 2178, p. 20150194, Jun. 2015.

[4] K. Bobzin, M. Öte, M. A. Knoch, I. Alkhasli, and H. Heinemann, "High-speed video analysis of the process stability in plasma spraying," *J. Therm. Spray Technol.*, vol. 30, pp. 987–1000, Feb. 2021.

[5] T. Senoo, A. Namiki, and M. Ishikawa, "High-speed batting using a multi-jointed manipulator," in *Proc. IEEE Int. Conf. Robot. Autom. (ICRA)*, New Orleans, LA, USA, Apr. 26-May 1, 2004, pp. 1191–1196.

[6] S. Morikawa, T. Senoo, A. Namiki, and M. Ishikawa, "Real-time collision avoidance using a robot manipulator with light-weight small high-speed vision systems," in *Proc. IEEE Int. Conf. Robot. Autom. (ICRA)*, Rome, Italy, Apr. 10-14, 2007, pp. 794–799.

[7] K. Ito, T. Sueishi, Y. Yamakawa, and M. Ishikawa, "Tracking and recognition of a human hand in dynamic motion for janken (rock paper-scissors) robot," in *Proc. IEEE Int. Conf. Autom. Sci. Eng. (CASE)*, Fort Worth, TX, USA, Aug. 21-25, 2016, pp. 891–896.

[8] S. Huang, Y. Yamakawa, T. Senoo, and M. Ishikawa, "Dynamic compensation by fusing a high-speed actuator and high-speed visual feedback with its application to fast peg-and-hole alignment," *Adv. Robot.*, vol. 28, no. 9, pp. 613–624, Feb. 2014.

[9] H. Arita, "A fast optical proximity sensor skin that contains an analog computing circuit and can cover an entire link," *Adv. Robot.*, vol. 37, no. 17, pp. 1083–1099, Jul. 2023.

[10] H. Hasegawa, Y. Suzuki, A. Ming, K. Koyama, M. Ishikawa, and M. Shimojo, "Net-Structure Proximity Sensor: High-speed and free-form sensor with analog computing circuit," *IEEE/ASME Trans. Mechatron.*, vol. 20, no. 6, pp. 3232–3241, Dec. 2015.